10.1098/rsta.2000.0809

THE ROYAL SOCIETY

Interactions and phase transitions of colloidal dispersions in bulk and at interfaces

By H. Löwen, E. Allahyarov, J. Dzubiella, C. von Ferber, A. Jusufi, C. N. Likos and M. Heni

Institut für Theoretische Physik II, Heinrich-Heine-Universität Düsseldorf, D-40225 Düsseldorf, Germany

Recent progress in the theory and computer simulation of effective interactions and phase transitions of colloidal dispersions is reviewed. Particular emphasis is put on the role of the discrete solvent in determining the effective interaction between charged colloids, bulk fluid–fluid phase separation of star-polymer–colloid mixtures, and on interfacial freezing transitions of sterically stabilized colloids on patterned substrates.

Keywords: effective interaction; charged colloids; star polymers; phase separation; surface freezing

1. Introduction

Colloidal dispersions represent excellent model systems with a clear separation of length-scales between microscopic degrees of freedom (such as solvent particles, counter- and salt-ions, monomers of grafted polymer chains, etc.) and the mesocopically sized colloidal particles. Typically, one is only interested in colloidal properties such as, for example, structural correlations or phase transitions of the colloidal particles. In this case, only thermodynamic averages with respect to the microscopic degrees of freedom are needed, resulting in effective interactions between the colloids. In this paper, we apply this concept to different situations of colloidal science, highlighting recent progress in the theory and computer simulation of effective interactions between charged colloidal suspensions, as well as mechanisms of fluid–fluid phase separation in mixtures of colloids and polymers. Finally, we also address interfacial freezing transitions induced by a periodic substrate pattern.

The paper is organized as follows. The role of a molecular solvent on the effective interactions is emphasized in § 2. The effective interactions in star-polymer–colloid mixtures and their impact on fluid–fluid phase separation are briefly sketched in § 3. Finally, we describe recent results on surface freezing of neutral colloidal particles on topographically structured templates in § 4, and conclude in § 5.

2. Influence of a granular solvent on the effective interaction between charged colloids

(*a*) *General remarks: modelling on different levels*

Basically, the theoretical model for the description of charged colloidal particles can be done on five different levels (for a recent review, see Hansen & Löwen (2000)).

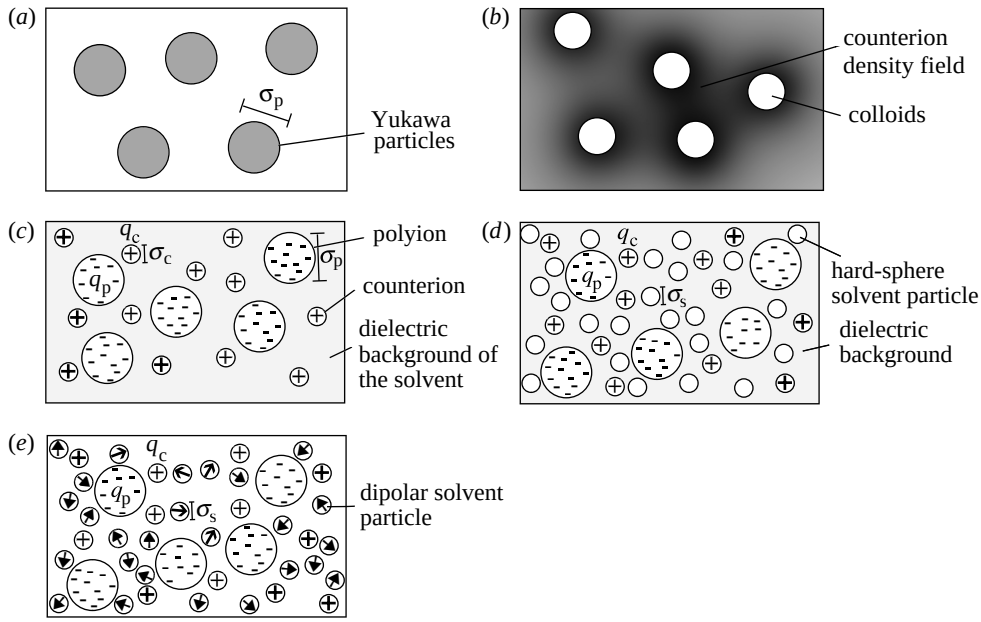

Figure 1. Different levels for the modelling of spherical charged colloidal particles. (*a*) level 1, DLVO; (*b*) level 2, PB; (*c*) level 3, PM; (*d*) level 4, hard-sphere solvent model; (*e*) level 5, dipolar solvent. For further explanation, see the text.

The higher the level, the more realistic the model is, and, at the same time, the more complicated the computational effort. Any higher level includes the lower levels as special cases. This is shown schematically in figure 1.

(1) The simplest approach is the linear counterion screening theory, which results in an analytical Yukawa pair potential for the effective interaction between colloids, as given by the electrostatic part of the celebrated Derjaguin–Landau–Verwey–Overbeek (DLVO) theory (Derjaguin & Landau 1942; Verwey & Overbeek 1948). In the absence of added salt, this potential, as a function of the distance between a colloidal pair, reads

$$V(r) = \frac{q_{\mathrm{p}}^2 \exp(-\kappa(r-\sigma_{\mathrm{p}}))}{(1+\frac{1}{2}\kappa\sigma_{\mathrm{p}})^2 \epsilon r}, \tag{2.1}$$

with an inverse Debye–Hückel screening length $\kappa = \sqrt{4\pi\rho_{\mathrm{c}} q_{\mathrm{c}}^2/\epsilon k_{\mathrm{B}}T}$. Here, q_{p} (q_{c}) is the polyion (counterion) charge, σ_{p} is the polyion radius, and ϵ is the dielectric constant of the solvent. Furthermore, ρ_{c} is the counterion bulk number density and $k_{\mathrm{B}}T$ is the thermal energy. On this level, only the colloidal particles are considered explicitly.

(2) The next level is the nonlinear *Poisson–Boltzmann* (PB) approach, which includes a full treatment of the counterion entropy but still works on a mean-field level. By a suitable linearization, one recovers the DLVO theory as a special case. On the PB level, the colloids and the averaged counterion density field are considered explicitly.

(3) In the *'primitive' model* (PM), one treats the counterions explicitly, arriving at the two-component model of strongly asymmetric electrolytes. The number density of the counterions is linked by global charge neutrality to the polyion charge and number density. This approach includes full counterion correlations. Ignoring these, the PM reduces to the PB level. The solvent, on the other hand, only enters via a continuous dielectric background. In detail, the input pair potentials are

$$V_{ij}(r) = \begin{cases} \infty & \text{for } r \leqslant \frac{1}{2}(\sigma_i + \sigma_j), \\ q_i q_j / \epsilon r & \text{otherwise,} \end{cases} \tag{2.2}$$

with $(ij) = (\mathrm{pp})$, (pc), (cc), and σ_c denoting the diameter of the counterions.

(4) If the solvent is treated explicitly, but only crudely modelled as neutral hard spheres of diameter σ_s, one arrives at the so-called *hard-sphere solvent model* (HSSM). This level includes the discrete molecular structure of the solvent (its granularity), but ignores its polarizability, as well as all its multipole moments (Kinoshita *et al.* 1996). Still, the dielectricity of the solvent is treated as a continuous background. In the limit $\sigma_\mathrm{s} \to 0$, the solvent is a decoupled ideal gas and one gets the PM as a special case. The interactions on this level are the same as in (2.2), but now with $(ij) = (\mathrm{pp})$, (pc), (ps), (cc), (cs), (ss), where the solvent is neutral, $q_\mathrm{s} \equiv 0$.

(5) Finally, one may describe the polar solvent with a permanent dipole moment. A suitable model is hard-sphere dipoles, the so-called *dipolar solvent model* (Lado 1997; Weis 1998) or a Stockmayer liquid (Groh & Dietrich 1994, 1995). On this level, the screening of the Coulomb interactions (i.e. the dielectric constant ϵ) is an output and not an input. With quantum chemistry, one may even reach a higher level with a full microscopic description of the solvent interactions (Marx 1999; Marx *et al.* 2000).

We note that there are two important 'intermediate' cases. First, nonlinear screening effects resulting from PB theory can be partly incorporated into a Yukawa potential similar to (2.1), but with 'renormalized' parameters leading to the concept of colloidal *charge renormalization*, as quantitatively elaborated by Alexander *et al.* (1984). We call this approach the *Poisson–Boltzmann–Yukawa model* (PBYM).

Hence this approach is between levels 1 and 2. It is consistent with experimental data in dilute bulk solutions with monovalent counterions (Härtl & Versmold 1988; Palberg *et al.* 1995; Crocker & Grier 1994; Grier 1998; Kepler & Fraden 1994). Second, one may consider the *solvent-averaged primitive model* (SPM) by tracing out the hard-sphere solvent exactly from level 4 and approximately only include the pairwise part, similar to the old McMillan–Mayer approach for electrolyte solutions (McMillan & Mayer 1945). The SPM includes solvent-depletion forces (Biben *et al.* 1996; Dickman *et al.* 1997; Dijkstra *et al.* 1998, 1999; Götzelmann *et al.* 1999) on the pairwise level, in addition to the traditional PM interactions, but the solvent particles are not considered explicitly.

(*b*) *Comparison of the HSSM with the PM*

In almost any theoretical study (Allahyarov *et al.* 1998; Linse & Lobaskin 1999; Messina *et al.* 2000) of the effective interaction between charged colloids, the PM

was used. The reason for this modelling is that the effective interaction is studied for mesoscopic distances between the colloids, where one could expect that the molecular nature of the neutral solvent averages out and only the long-ranged Coulomb interaction may play the dominant role. A more subtle inspection shows, however, that the solvent may have an important influence by pushing counterions towards the colloidal surface via hydration forces. One may still believe in the PM by reducing the colloidal charge q_{p} by the amount of counterions accumulated on the colloidal surfaces and treating only the rest explicitly as mobile counterions within the PM. Still, this separation into fixed and mobile counterions is questionable as the counterions are highly correlated near the polyionic surfaces.

We have tested the validity of the PM by doing extensive computer simulations on the higher level 4 using the HSSM. These require an enormous number of solvent particles, so that one is restricted to moderate size asymmetries between colloidal and solvent spheres. Together with a solvent bath method, which is described elsewhere (Allahyarov & Löwen 2001), one can achieve size asymmetries of 14:1 at significant solvent-packing fractions corresponding to charged micelles. Explicit results for the averaged force $F(r)$ between a pair of charged polyions as a function of their mutual distance r are presented in figure $2a, b$. The parameters are $T = 298\,\mathrm{K}$ and $\epsilon = 81$ (water at room temperature), with $\sigma_{\mathrm{s}} = 3\,\text{Å}$, $\phi_{\mathrm{s}} = 0.3$ and $\sigma_{\mathrm{c}} = 6\,\text{Å}$.

For nearly touching polyions (full curves in the insets of figure 2), the force exhibits oscillations on the scale of the solvent diameter due to solvent layering leading to attraction for touching polyions as the solvent depletion part exceeds the bare Coulomb repulsion. For larger distances and monovalent counterions, the force is repulsive. Simulation data for the PM are also included which overestimate the force. The repulsion is even stronger in the PBYM and in DLVO theory. For divalent counterions, on the other hand, there is attraction within a range of several polyion diameters. This attraction is mediated by the discrete solvent as the PM yield repulsive forces. The SPM, on the other hand, almost perfectly fits the simulation data and thus includes the essential effects of the discrete solvent. As expected, the PBYM and the DLVO theory overestimate the force and do not lead to attraction.

In conclusion, although the interaction range of a hard-sphere solvent is small, the depletion attraction of the counterions towards the colloidal surfaces favours an accumulation of counterions near the polyions. This, in turn, leads to a different screening, resulting in a different long-range part of the colloid–colloid interaction. For divalent counterion, even over-screening may occur, leading to attraction. This attraction is absent in the PM.

3. Phase separation in star-polymer–colloid mixtures

We now turn to an example of a bulk phase transition, in particular to fluid–fluid phase separation in mixtures of neutral sterically stabilized particles and star polymers in a good solvent. We aim at a description on the level of two particle species having integrated out the monomer (and solvent) degrees of freedom.

The corresponding effective potentials are determined by a computer simulation of two particles. The colloid–colloid interaction is hard-sphere like,

$$V_{\mathrm{cc}}(r) = \begin{cases} \infty & \text{for } r \leqslant \sigma_{\mathrm{coll}}, \\ 0 & \text{otherwise}, \end{cases} \tag{3.1}$$

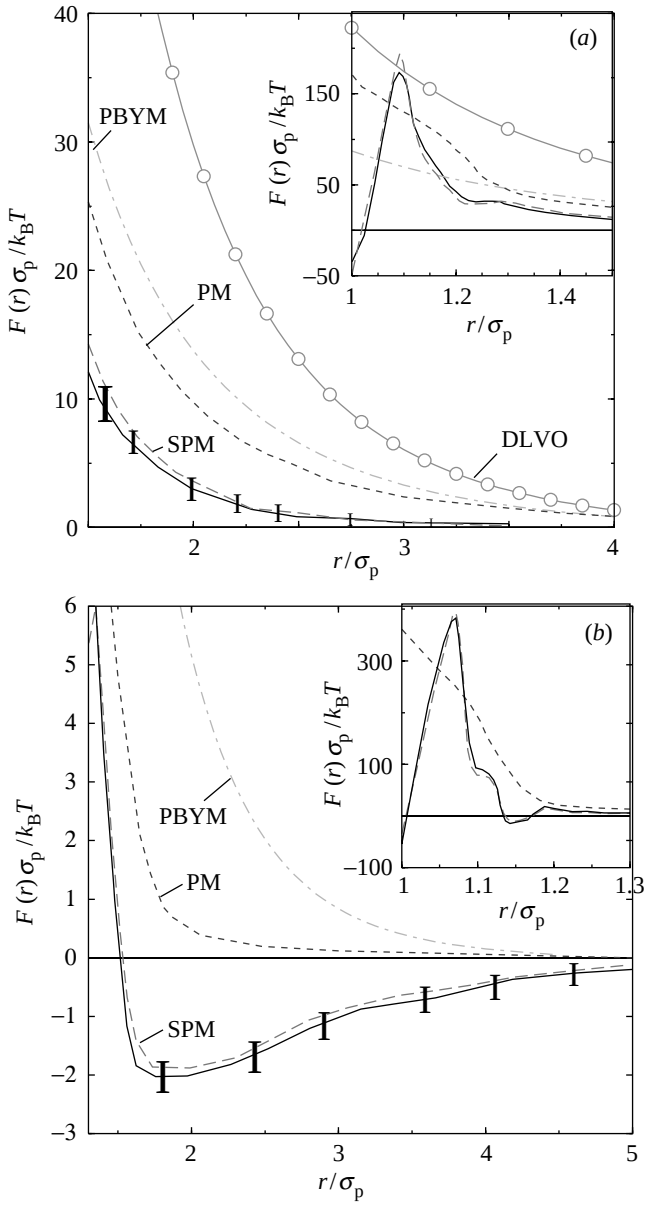

Figure 2. Reduced distance-resolved force $F(r)\sigma_p/k_BT$ versus reduced distance r/σ_p. The inset shows the same for nearly touching polyions of molecular distances. (*a*) Monovalent counterions and σ_p:σ_c:σ_s = 10:2:1. (*b*) Divalent counterions and σ_p:σ_c:σ_s = 14:2:1. The further parameters are $|q_p/q_c| = 32$ and $\phi_p = 5.8 \times 10^{-3}$. Solid line with error bars, full solvent bath simulation; long-dashed line, SPM; short-dashed line, PM; open circles, DLVO theory; dot-dashed line, PBYM.

where σ_{coll} is the colloid diameter. The star–star interaction has been the focus of intense recent research. By molecular simulation resolving the monomers explicitly (Jusufi *et al*. 1999) and by theoretical scaling arguments and neutron scattering data,

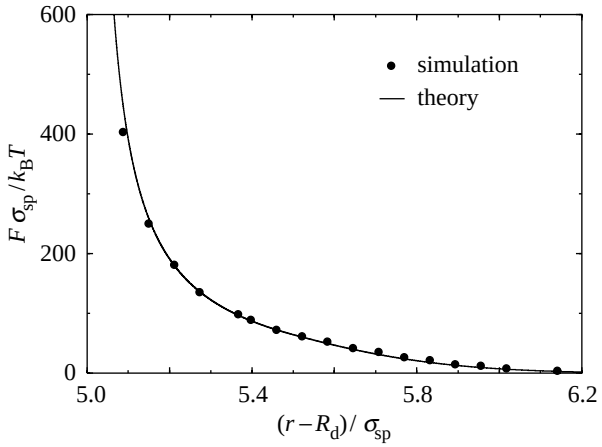

Figure 3. Force between a star polymer and a hard sphere for an arm number $f = 32$ and size ratio $q = \sigma_{sp}/\sigma_{coll} = 0.1$. The points are results from a molecular simulation, fitted with the theoretical force (line) corresponding to (3.3). With R_d, a non-vanishing core size of the simulated star is subtracted.

a simple analytical form for the effective star–star interaction was derived. It reads (Likos *et al.* 1998)

$$V_{ss}(r) = \tfrac{5}{18} k_B T f^{3/2} \begin{cases} -\ln\left(\dfrac{r}{\sigma_{sp}}\right) + \dfrac{1}{1+\frac{1}{2}\sqrt{f}} & \text{for } r \leqslant \sigma_{sp}, \\ \dfrac{1}{1+\frac{1}{2}\sqrt{f}}\left(\dfrac{\sigma_{sp}}{r}\right)\exp\left(-\dfrac{\sqrt{f}}{2\sigma_{sp}}(r-\sigma_{sp})\right) & \text{otherwise,} \end{cases} \tag{3.2}$$

and was used to calculate the bulk phase diagram of star polymers (Watzlawek *et al.* 1999). Here, σ_{sp} is the corona diameter and f the arm number of the stars. This potential was generalized recently to two different arm numbers (von Ferber *et al.* 2000*a*) and triplet interactions have been shown to be small in semi-dilute star-polymer solutions (von Ferber *et al.* 2000*b*). The major problem is a quantitative description of the star-polymer–colloid interaction. We have again used molecular simulation to obtain the effective force acting on a star polymer near a hard sphere. The averaged force as a function of the colloid–star-polymer separation is presented in figure 3. The corresponding effective potential, in turn, is well described by an analytical function of the form

$$V_{sc}(r) = \lambda k_B T f^{3/2} \frac{\sigma_{coll}}{2r} \begin{cases} \infty & \text{for } r < \frac{1}{2}\sigma_{coll}, \\ -\ln\left(\dfrac{2z}{\sigma_{sp}}\right) - \left(\dfrac{4z^2}{\sigma_{sp}^2} - 1\right)(\xi_1 - \tfrac{1}{2}) + \xi_2 & \text{for } \tfrac{1}{2}\sigma_{coll} \leqslant r < \tfrac{1}{2}(\sigma_{sp}+\sigma_{coll}), \\ \dfrac{\xi_2(1-\mathrm{erf}(2\kappa z))}{1-\mathrm{erf}(\kappa\sigma_{sp})} & \text{otherwise,} \end{cases} \tag{3.3}$$

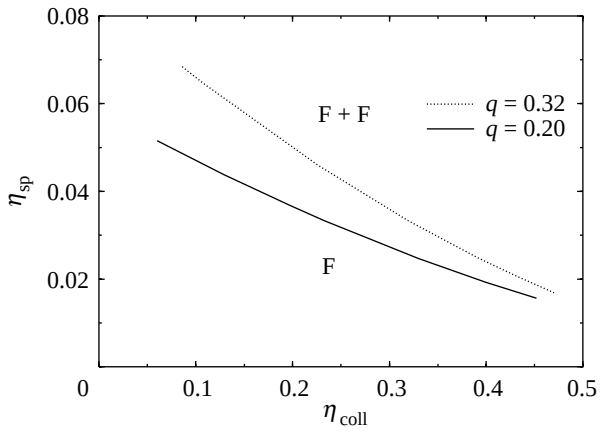

Figure 4. Binodals for the mixing–demixing transition in a star-polymer–colloid mixture for two different size ratios $q = \sigma_{sp}/\sigma_{coll}$ and an arm number $f = 32$. η_i with $i = \mathrm{sp}, \mathrm{coll}$ defines the packing fraction of the particles.

where $z = r - \frac{1}{2}\sigma_{coll}$ is the distance from the centre of the star polymer to the surface of the colloid. The constants are

$$\xi_1 = \frac{1}{1 + 2\kappa^2\sigma_{sp}^2} \quad \text{and} \quad \xi_2 = \frac{\sqrt{\pi}\xi_1}{\kappa\sigma_{sp}} \exp(\kappa^2\sigma_{sp}^2)(1 - \mathrm{erf}(\kappa\sigma_{sp})),$$

while λ and κ are fit parameters. The radius of gyration is $R_g = \sigma_{sp}/1.32$, fixed for all arm numbers f and size ratios $q = \sigma_{sp}/\sigma_{coll}$. Taking these three potentials as an input, we have employed the Rogers–Young closure scheme to access the liquid structure and the thermodynamics of the star-polymer–colloid mixture. A fluid–fluid phase separation was found, which is shown for an arm number of $f = 32$ in figure 4. This picture is consistent with recent experimental data (Dzubiella *et al*. 2001). Star polymers are hybrid objects between hard-sphere colloids and coils of linear polymer chains such that one can continuously switch between these two cases by changing the arm number f. While in hard-sphere mixtures the fluid–fluid phase separation is preempted by freezing (Dijkstra *et al*. 1998), it is stable for linear polymer chains (Lekkerkerker *et al*. 1992) for suitably large polymer coils. Our case of star polymers is intermediate but still exhibits fluid–fluid phase separation.

4. Surface freezing of colloids on periodically patterned substrates

Phase transitions can also occur at interfaces. For example, there is a wealth of wetting phenomena (Evans 1990; Dietrich 1988). One peculiar case is the surface freezing transition. For hard-sphere colloids, it has been shown that a hard structureless wall induces precrystallization, i.e. few crystalline layers on top of the wall show up, even if the bulk density is below the freezing point of the fluid (Courtemanche & van Swol 1992; Courtemanche *et al*. 1993). The question we address in this section is whether and how this prefreezing effect is influenced by a topographically periodic surface pattern. We model this pattern by a periodic array of fixed hard spheres on a two-dimensional triangular or rhombic lattice. In fact, by 'gluing' colloidal spheres onto a periodic pattern, such surface structures can indeed be realized experimentally

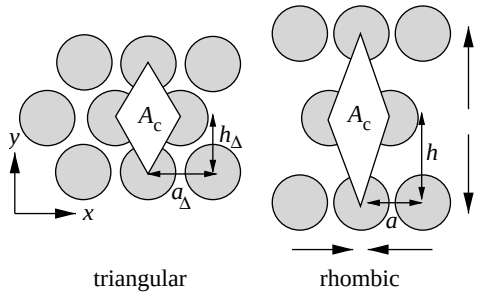

Figure 5. Geometry of the triangular and rhombic substrate pattern consisting of fixed hard spheres in a plane. The rhombic pattern results from the triangular one by distorting the lattice, as indicated by the arrows, such that the area A_c of the unit cell remains constant.

(Arora & Rajagopalan 1997; van Blaaderen *et al*. 1997; Burmeister *et al*. 1997; Mio & Marr 1999).

The surface structure is sketched in figure 5. A triangular crystal that exactly fits the bulk face-centred cubic crystal coexisting with the fluid at the bulk freezing point is used as one possible substrate pattern. We also consider patterns that are distorted such that the area A_c of the unit cell does not change. In detail, in the triangular case, the lattice constant a_Δ is 1.1075σ (σ denoting the hard-sphere diameter), with a height h_Δ. The rhombic pattern has a lattice constant a smaller than a_Δ, but a larger height h. We characterize the rhombic distortion via the lateral strain

$$\epsilon_\parallel = \sqrt{\left(\frac{a-a_\Delta}{a_\Delta}\right)^2 + \left(\frac{h-h_\Delta}{h_\Delta}\right)^2}.$$

Hence the whole system is completely characterized by the reduced bulk hard-sphere pressure $P^* = P\sigma^3/k_BT$ and the lateral strain $\epsilon_\parallel$. Monte Carlo simulations with suitable-order parameters (Heni & Löwen 2000) are used to detect freezing in different layers adjacent to the wall. We find a cascade of freezing transitions in the different layers. There is complete surface freezing for the triangular substrate. Complete freezing is possible as there is no additional strain that hinders growth of a full bulk solid upon approaching coexistence. The onset of surface freezing in the first adjacent layers occurs already at bulk pressures P^* that are 29% smaller than the coexistence pressure P_c^*, while the onset of precrystallization for a flat wall occurs at pressures that are only *ca.* 3% smaller than P_c^*. For a rhombic pattern, on the other hand, surface freezing is incomplete, since the additional lateral strain results in a free energy penalty, which prevents further growth of the crystalline layers. The resulting crystalline phase inherits its structure directly from the underlying substrate pattern and is unstable as a bulk phase.

Our simulation results are summarized in figure 6, where the location of the first four layering transitions is shown in the plane spanned by $\Delta P^* = P_c^* - P^*$ and $\epsilon_\parallel^2$. A simple phenomenological approach that combines elasticity theory of the solid with thermodynamic arguments of wetting (Heni & Löwen 2000) yields a linear relation between ΔP^* and $\epsilon_\parallel^2$ for the freezing transitions in the same layer. The slope can be expressed by elastic constants and thermodynamic quantities. This simple theory fits the simulation data quite well. If the lateral strain $\epsilon_\parallel$ exceeds a critical value, there is no surface crystallization at all, since the elastic distortion is too large to produce

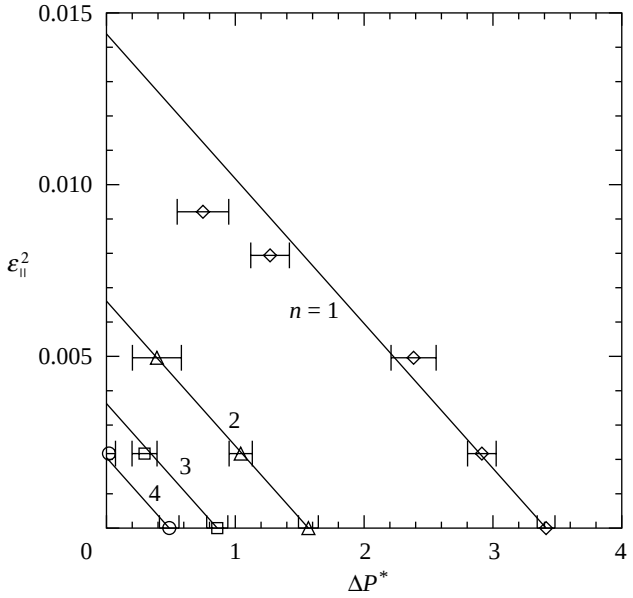

Figure 6. Location of the first four layering transitions in the plane spanned by ΔP^* and $\epsilon_{\|}^2$. The symbols represent simulation data with their statistical error. The straight lines are the theoretical predictions. The deviation between simulation and theory for high $\epsilon_{\|}^2$ in the first layer is due to harmonic elastic effects that are not accounted for in the theory.

even a single crystalline layer. The system prefers to stay in the inhomogeneous fluid phase in this case.

In conclusion, the structure of a substrate pattern profoundly influences the scenario of surface freezing. First, the onset of surface freezing can be significantly shifted away from coexistence by using a pattern that favours the crystal, as the triangular pattern in our study shows. Second, new surface phases, which are unstable as bulk phases, can be generated by a suitable pattern, leading to incomplete freezing at coexistence, as demonstrated for the rhombic pattern in our study. Third, surface freezing can be completely suppressed if the pattern is unfavourable for the solid.

5. Conclusion and outlook

To summarize, the concept of the effective potential can be exploited to bridge the length-scale gap omnipresent in colloidal applications, where the mesoscopic colloidal particles are coupled to many microscopic degrees of freedom. Once the effective potential is known, one may employ classical many-body theories (e.g. liquid integral equation schemes) or ordinary computer simulations to access the structural correlations or phase transitions in colloidal dispersions. The big advantage over molecular systems is that everything is shifted to a larger length-scale, so that real-space methods can be applied experimentally and so that controlled external perturbations such as well-characterized periodic substrate patterns can be realized. In this respect, colloidal dispersions play an important role as model systems subject to externally controllable fields.

References

Alexander, S., Chaikin, P. M., Grant, P., Morales, G. J., Pincus, P. & Hone, D. 1984 *J. Chem. Phys.* **80**, 5776.

Allahyarov, E. & Löwen, H. 2001 *J. Phys. Condens. Matter* **13**, L277.

Allahyarov, E., D'Amico, I. & Löwen, H. 1998 *Phys. Rev. Lett.* **81**, 1334.

Arora, A. K. & Rajagopalan, R. 1997 *Curr. Opin. Colloid Interface Sci.* **2**, 391.

Biben, T., Bladon, P. & Frenkel, D. 1996 *J. Phys. Condens. Matter* **8**, 10 799.

Burmeister, F., Schäfle, C., Matthes, T., Bohmisch, M., Boneberg, J. & Leiderer, P. 1997 *Langmuir* **13**, 2983.

Courtemanche, D. J. & van Swol, F. 1992 *Phys. Rev. Lett.* **69**, 2078.

Courtemanche, D. J., Pasmore, T. A. & van Swol, F. 1993 *Molec. Phys.* **80**, 861.

Crocker, J. C. & Grier, D. G. 1994 *Phys. Rev. Lett.* **73**, 352.

Derjaguin, B. V. & Landau, L. D. 1942 *Acta Physiochim. USSR* **14**, 633.

Dickman, R., Attard, P. & Simonian, V. 1997 *J. Chem. Phys.* **107**, 205.

Dietrich, S. 1998 *Phase transitions and critical phenomena* (ed. C. Domb & J. L. Lebowitz), vol. 12, pp. 1–128. Academic.

Dijkstra, M., van Roij, R. & Evans, R. 1998 *Phys. Rev. Lett.* **81**, 2268.

Dijkstra, M., van Roij, R. & Evans, R. 1999 *Phys. Rev. Lett.* **82**, 117.

Dzubiella, J. (and 11 others) 2001. (In preparation.)

Evans, R. 1990 *Liquids at interfaces, Les Houches Session XLVIII* (ed. J. Charvolin, J. F. Joanny & J. Zinn-Justin). Elsevier.

Götzelmann, B., Roth, R., Dietrich, S., Dijkstra, M. & Evans, R. 1999 *Europhys. Lett.* **47**, 398.

Grier, D. G. 1998 *Nature* **393**, 621.

Groh, B. & Dietrich, S. 1994 *Phys. Rev. Lett.* **72**, 2422.

Groh, B. & Dietrich, S. 1995 *Phys. Rev. Lett.* **74**, 2617.

Hansen, J. P. & Löwen, H. 2000 *Ann. Rev. Phys. Chem.* **51**, 209–242.

Härtl, W. & Versmold, H. 1988 *J. Chem. Phys.* **88**, 7157.

Heni, M. & Löwen, H. 2000 *Phys. Rev. Lett.* **85**, 3668.

Jusufi, A., Watzlawek, M. & Löwen, H. 1999 *Macromolecules* **32**, 4470.

Kepler, G. M. & Fraden, S. 1994 *Phys. Rev. Lett.* **73**, 356.

Kinoshita, M., Iba, S. & Harada, M. 1996 *J. Chem. Phys.* **105**, 2487.

Lado, F. 1997 *J. Chem. Phys.* **106**, 4707.

Lekkerkerker, H. N. W., Poon, W. C.-K., Pusey, P. N., Stroobants, A. & Warren, P. B. 1992 *Europhys. Lett.* **20**, 559–564.

Likos, C. N., Löwen, H., Watzlawek, M., Abbas, B., Jucknischke, Allgaier, J. & Richter, D. 1998 *Phys. Rev. Lett.* **80**, 4450–4453.

Linse, P. & Lobaskin, V. 1999 *Phys. Rev. Lett.* **83**, 4208.

McMillan, W. G. & Mayer, J. E. 1945 *J. Chem. Phys.* **13**, 276.

Marx, D. 1999 In *New approaches to problems in liquid state theory* (ed. C. Caccamo, J. P. Hansen & G. Stell), NATO ASI Series, vol. 529, Dordrecht: Kluwer Academic.

Marx, D., Tuckerman, M. E. & Parrinello, M. 2000 *J. Phys. Condens. Matter* **12**, 153.

Messina, R., Holm, C. & Kremer, K. 2000 *Phys. Rev. Lett.* **85**, 872.

Mio, C. & Marr, D. W. M. 1999 *Langmuir* **15**, 8565.

Palberg, T., Mönch, W., Bitzer, F., Piazza, R. & Bellini, T. 1995 *Phys. Rev. Lett.* **74**, 4555.

van Blaaderen, A., Ruel, R. & Wiltzius, P. 1997 *Nature* **385**, 321.

Verwey, E. J. W. & Overbeek, J. T. G. 1948 *Theory of the stability of lyophobic colloids.* Elsevier.

von Ferber, C., Jusufi, A., Watzlawek, M., Likos, C. N. & Löwen, H. 2000*a* *Phys. Rev.* E **62**, 6949–6956.

von Ferber, C., Jusufi, A., Likos, C. N., Löwen, H. & Watzlawek, M. 2000*b* *Eur. Phys. J.* E **2**, 311–318.

Watzlawek, M., Likos, C. N. & Löwen, H. 1999 *Phys. Rev. Lett.* **82**, 117.

Weis, J. J. 1998 *Molec. Phys.* **93**, 361.

Discussion

S. Safran (*Weizmann Institute of Science, Rehovot, Israel*). One might be able to relate the increasing complexity of four various 'levels' and the observation that the interactions become more attractive as more detailed levels are calculated by noting that higher levels include *more* degrees of freedom.

The inclusion of additional degrees of freedom *must* lower the free energy (or else those degrees of freedom would just be 'frozen out'). The *decrease* of free energy may result in the increasing *attractions* (one would expect expulsions to increase the free energy), but this argument is not yet rigorous.

H. Löwen. Indeed, if one includes more degrees of freedom, the total free energy goes down. This, however, does not imply that *derivatives* of the total free energy, with respect to some parameters, will also decrease. The effective force is such a derivative. In fact, one can find a simple counterexample in which, by adding additional degrees of freedom, even repulsions in the effective force can arise. This is the case for a binary mixture of hard spheres: with only one component, the effective interaction is zero outside the core. With small spheres added, there is an oscillatory depletion interaction, which can be both attractive and repulsive.

H. H. von Grünberg (*Fachbereich Physik, Universität Konstanz, Germany*). In figure 1 you summarized the different models/approximations for an inhomogeneous electrolyte solution: (a) Debye–Huckel approximation (DH), (b) Poisson–Boltzmann (PB), (c) primitive model, (d) hard spheres for water molecules, and (e) hard-spheres plus dipoles for water. Each of these five levels is understood to be an improvement of the previous level; so, PB improves on DH, primitive model on PB, and so forth. This means that you assume that a description of water as hard spheres with a dipole moment (level (e)) is an improvement of the simple hard-sphere model for water, thus implying that the steric effect of water molecules is more important than effects caused by the dipole moments of water. Would one not expect that it is just the other way round, i.e. the permanent dipole each water molecule has is a much more important property than the mere steric effect of water accounted for by the hard-sphere model? The first step to improve on a primitive model calculation would then be a model where one takes account of the most prominent property of water, namely that it is a strong dipole.

H. Löwen. How to include real water in a realistic way in order to 'improve' the primitive model is still a debate. Of course, the dipolar moment will be important. In fact, as the dipolar moment results in a long-ranged interaction while a steric interaction is short ranged, the dipole moment is much more important for a *dilute* solvent. In a dense liquid, on the other hand, one might expect that the dipolar nature averages out, establishing a nearly homogeneous dielectric background, and that thus the excluded volume of the solvent molecules is the most prominent property. Still more microscopic work is needed to clarify this issue.

C. W. Outhwaite (*School of Mathematics, University of Sheffield, UK*). On one of your overheads you said the granular (or solvent) primitive model is justified. Could you please explain how, as the status of this model between the McMillan–Mayer and Born–Oppenheimer description levels (figure 1), is to my knowledge not clearly not understood at the statistical mechanical level.

H. Löwen. What I claimed was that the SPM was justified by comparing its predictions to the full granular solvent model. This SPM corresponds exactly to the McMillan–Mayer description level.